A Study of The Electronic State in W–Cu Alloys

Mohammed Nazar Mohammed[1*]

[1] *Salahdeen Education Directorate, Department of Alduluiya Education , Salahaddin ,IRAQ*

[*] *Corresponding Author:* moh.nz.2023@gmail.com

Received 16 march. 2024, Accepted 20 June. 2025, published 30 Dec. 2025.

DOI: 10.52113/2/12.02.2025/1-13

ABSTRACT: The quantum theory of scattering of electromagnetic waves by charged particles is known as Compton effect which can give us valuable information about the electronic structure of transition metals and alloys. In this study it was calculated the Electronic State for two (W-Cu) alloys, where Compton profile (CP) for W, Cu elements it was calculated theoretically by using the Renormalized Free Atom (RFA) model, The study found that the best electronic configuration for the two elements is: ($5d^{5}$-$6s^{1}$) and ($3d^{9.9}$-$4s^{1.1}$) respectively after has been compared the results that have been obtained with the available experimental values, Free atom (FA) data has also been added for two elements in the study. Also found Compton profile (CP) for the two alloys ($W_{60\%}$-$Cu_{40\%}$),($W_{72\%}$-$Cu_{28\%}$) using the Superposition model and the results were compared with the available experimental values and Augmented Plane Wave (APW) data respectively. the calculations theoretical for Superposition model was give a better agreement with available experimental values.

Keywords: Compton profile(CP), The Renormalized Free-Atom model, (Superposition) model, Compton scattering, alloys.

1. Introduction

The inter-transition metal binary alloys are of special interest because the valence band d electrons play important role in their physical and electronic properties. In experimental and theoretical physics the electronic characteristics of W-Cu system are of interest because of its many applications like including fusion reactors, microelectronics, and military ordnance applications, which made for this alloy a subject of scientific and technological interest. The electronic structure of W-Cu along with some other transition-metal alloys has been investigated by[1].These authors have compared their empirical results with (Sup) model and band structure calculations[2].The W-Cu system that consists mainly of two intermetallic alloys i.e. ($W_{60\%}$-$Cu_{40\%}$),($W_{72\%}$-$Cu_{28\%}$) However, attempts to study the properties of the ground state such as the distribution momentum density by the Compton profile have not been made theoretically, as far as know, for any configuration of the (W-Cu) system, Therefore, in our study, discussed the study EMD (theoretically) in alloys (W-Cu) by the Compton profile. The process of interaction of radiation with matter occurs mainly through Compton scattering, which was discovered in 1923 by theoretical interpretations of the x-ray experiment[3]. Historically, the discovery of

gamma rays and x-rays by Roentgen gave rise to the Compton effect[4]. When inelastic scattering of x-rays by electrons occurs in solids, the energy distribution of the scattering photon has a Doppler broadened due to the momentum distribution of the electrons[5].From through a Doppler shift of scattered photons for Compton ,the momentum distribution of electrons in a material is measured by electrons in motion also a study of bonding electrons behavior can be made by studying the valence Compton profiles[6]. When an increase in the field occurs, the Compton effect is transmitted to the nonlinear system, and as a result, several photons are absorbed and converted into photons of high energy[7]. Also, the Compton scattering (CS) is a unique style and has multiple uses to test the correlation energies in matter by studying the electron momentum density[8].The EMD is a ground state property and thus useful for compares with theoretical calculations as the compute of response functions[9].Inelastic x-ray scattering at high energy and momentum transfers. The Compton profile allows verifying the quality of the electron wave functions through Fourier transforms, defining the Fermi surface and verifying the quality of band structure calculations[10]. Compton Profiles are widely used to analyze data on the electronic structure of a target material and have many applications in materials science, atomic physics, and condensed matter physics[11]. The Compton scattering technique gives us information related to the EMD of the solids, because the shape of the Compton profile is sentient to the movement of external electrons in atoms that move slowly[12-13].The status of the J(PZ) line of the scattering Compton radiation is revealed through spectral analysis of this radiation and depending on the impulse approximation (IA) theory, This can be reduced to the ‘CP’[14]. The assumed time for the Compton scattering reaction to occur according to (IA) is so small that the initial and final electrons see the same constant potential. The Compton scattering technique has been well proven to be a technique that has many uses, including validate the exchange potential by the electron momentum density[15]. Through CS technology, and can perform tests for the electronic properties of materials[16]. The CS technique is a useful experimental method for measuring momentum density in molecular and condensed matter systems[17]. The inelastic type of during the collision of a photon with an electron, Compton scattering will occur and part of the photon energy is transferred to the electron[18]. The Compton technique gives a number of substantial advantages when compared to other spectrometers that include this regard[19]. When comparing Compton scattering with other complementary methods for test the electronic momentum density of materials, we find that it

has special advantages as well[20]. Compton profile J(Pz) can be defined as: can provide information about the projection of electronic momentum density on the scattering wave vector, Within the impulse approximation, J(Pz) is given by[21].

$J(P_Z) = \iint n(p) dP_x\, dP_y$

where P_x momentum component in the x Cartesian direction and P_y momentum component in the y Cartesian direction and the z direction is parallel to the resultant of the incident and scattered wave vectors, *n(p)* are the electronic momentum density. In previous years, a great effort has been made by researchers to study the electronic states of polycrystalline alloys such as: Ti-Cu[2], Fe-Ni[22], Ti-Al[23], Cr-Ni[24], Ti-Ni[25],(AgCl and AgBr)[26], (PbCl2 and PbBr2)[27] and Cr-Fe-Mn[28]. using Compton scattering technique. The aim of this study discusses of the Compton profile (theoretically):

1. An theoretical Compton profile of W , Cu measured using RFA Model.
2. the theoretical Compton profile of ($W_{60\%}$-$Cu_{40\%}$),($W_{72\%}$-$Cu_{28\%}$) alloys using the Superposition Model.
3. To compare our theoretical result with available experimental values and (APW) data.

2. Theoretical Calculations

2.1. Calculations (RFA) model

In this part of the study, adopted on the (RFA) model in our theoretical calculations to find the configuration of the electrons of the shells (5d-6s) of the element tungsten and (3d-4s) of the element copper in order to find the best electronic arrangement for them, and this model gives correct results and agrees well with the results of the available experimental values. This (RFA) model considers that the atom is not free , but confined to a particular cell in the solid[29]. The success and validity of the RFA model is clearly evident in the studies and research presented by researchers such as Hodges[30]. Also, this model gives completely correct results for the characteristics of the bund structure and also an explanation of cohesion in the transition metal series. the calculation starts from Hartree-Fock wave function contained in tables[31-32] which is truncated at the Wigner-Seitz radius(R_0) and renormalized to unity within this sphere to preserve the charge neutrality. The new wave function $R_{nl}(r)$ is given by.

$$R_{nl}(r) = \begin{cases} N_{nl}^{-2}\ R_{nl}^{atomic(r)} & r \le R_0 \\ 0 & r > R_0 \end{cases} \qquad \textbf{(1)}$$

Here $R_{nl}^{atomic(r)}$ is the atomic radial wave function for the state with quantum number $n\ and\ l\ and\ N_{nl}$ is defined by.

$$N_{nl}^{-2} = \int_0^{R_0} \left| R_{nl}^{atomic(r)} \right|^2 r^2 dr$$

(2) In this way, the solid will be composed of independent atoms and will be almost in the same state as the solid state was formed before these atoms were associated with each other. The successes achieved by the simple RFA model compared with the available experimental measurement results proved that this model gives correct and accurate results. The effect of renormalized of the wave function of the shell electrons s is large, as the maximum percentage of the electronic charge present within the Wigner-Seitz spherical shape is within the range of (5%). As for the electrons of the shell d, this percentage is about (95%). For this reason, the effect of the calibration process on it be small. Please note that this RFA model is used to find the Compton profile for element W , Cu and Free atom (FA) data has also been added are taken directly from tables[33].

2.2 Calculations (Sup) Model

Using the Compton profile for element W and Cu, can find the Compton profiles $J^{ab}(P_Z)$ for both alloys by the equation below[23].

$$J^{ab}(P_Z) = (1 - c)J^{a}(P_Z) + cJ^{b}(P_Z) \quad \textbf{(3)}$$

Where c is the atomic concentration of b atoms in the ab alloy. whereas $J^{a}(P_Z), J^{b}(P_Z)$ are the theoretical calculations for (CP) of W and Cu, respectively. The $J(P_Z)$ for ($W_{60\%}$-$Cu_{40\%}$),($W_{72\%}$-$Cu_{28\%}$) alloys are calculation using this equ.3. For comparison, the values of the Compton profiles extracted according to the (APW) method have been added, Our theoretical values for the Compton profiles for ($W_{60\%}$-$Cu_{40\%}$),($W_{72\%}$-$Cu_{28\%}$) alloys are normalized to (18.2915, 20.4190) e^- respectively.

3. Results and Discussion

3.1. The discussion results of (RFA)

Table 1 includes our theoretical results for the Compton profiles values extracted by the RFA model for the elements W and Cu, the Compton profiles values extracted by FA from Biggs tables[33], as well as the available experimental values. The momentum region is (0→5a.u.) for all existing values. With regard to the element W, note that the values of the Compton profiles (RFA) as well as FA in the momentum region located between (2→5a.u.) are almost similar, and the reason for this is due to the fact that the electrons in this region are the electrons of the core. Also in the momentum region located between (0 → 0.3a.u.), note that the FA values are greater than the RFA and experimental values. For the momentum region (0.3 → 0.6a.u.) , notice that the values of the two models (RFA, FA) are close to each other when compared with the experimental values, in the momentum region (0.7 → 0.8a.u.), notice that all values are convergent except for the value of (Expt. for W).and in the momentum region (1.0 →1.8a.u.), notice that the values of the two models (RFA, FA) are somewhat close to each other when compared with the available experimental values, and the same applies to the

Cu element. in this study Our theoretical values for the Compton profiles for W and Cu are normalized to (23.7239, 11.8123) e^-. Respectively.

Table1: Our theoretical Compton profile results for W , Cu were compared to the experimental values[1].These values were normalized to (23.7239, 11.8123) e^-. Respectively

P_z (a.u.)	$J(p_z)$ in (electron/a.u.)					
	TUNGSTEN (W)			COPPER (Cu)		
	Free atom (FA)[33]	Core+RFA $5d^5$-$6s^1$	Expt.[1]	Free atom (FA)[33]	Core+RFA $3d^{9.9}$-$4s^{1.1}$	Expt.[1]
0.0	11.2	9.394	9.21±0.0152	5.93	5.222	5.12±0.0099
0.1	10.9	9.333	9.15	5.76	5.212	5.11
0.2	10.1	9.241	9.06	5.37	5.161	5.06
0.3	9.32	9.109	8.93	4.94	5.069	4.97
0.4	8.64	8.925	8.75	4.6	4.947	4.85
0.5	8.17	8.435	8.52	4.38	4.484	4.72
0.6	7.85	8.197	8.28	4.24	4.332	4.56
0.7	7.59	7.95	8.03	4.14	4.171	4.39
0.8	7.34	7.673	7.75	4.05	4.009	4.22
1.0	6.80	6.989	7.06±0.0126	3.86	3.796	3.89±0.0082
1.2	6.22	6.296	6.36	3.62	3.654	3.58
1.4	5.65	5.732	5.79	3.36	3.422	3.29
1.6	5.15	5.237	5.29	3.07	3.13	3.01
1.8	4.74	4.782	4.83	2.79	2.839	2.73
2	4.40	4.444	4.44±0.0090	2.52	2.558	2.46±0.0058
3	3.49	3.554	3.55±0.0067	1.47	1.455	1.50±0.0039
4	2.86	2.843	2.84±0.0053	0.914	0.912	0.94±0.0026
5	2.24	2.242	2.24±0.0042	0.632	0.64	0.66±0.0019

In Figure1, which shows the comparison between the calculations values (theoretical) of the shape of the Compton profile $J(P_Z)$ for the extracted arrangement of the (W) element by adopting the (RFA) model and the experimental values of (FA) with the approved experimental values given in Table 1, where better note the equality and differences in the theoretical extracted values through the two models (RFA, FA) with experimental values, note that the values of the (RFA) model are somewhat closer to the experimental values compared to the free atom model (FA) in the momentum region (P_Z=2→5a.u) and The same applies to (Cu) , shown in Figure 2.

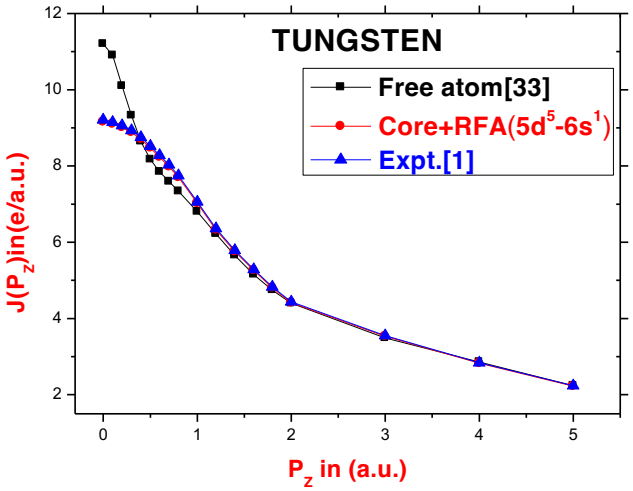

Fig.(1): Comparison Compton J(P_Z) profile of the our theoretical values with experimental values[1] for the element (W) ,all values were normalized to (23.7239) e^-.

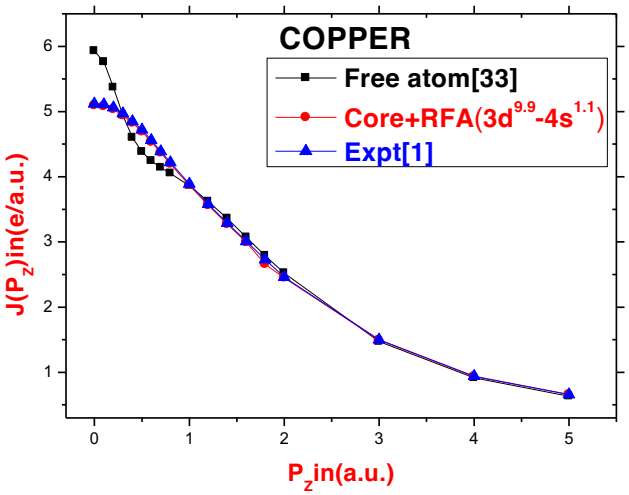

Fig.(2): Comparison Compton J(P_Z) profile of the our theoretical values with experimental values[1] for the element (Cu) ,all values were normalized to (11.8123) e^-.

3.2. The discussion results of (SUP)

The our theoretical results of the Compton J(P_Z) profile, which were obtained in the final form after all calculations and corrections were made, are given in Tables (2-3) for alloys ($W_{60\%}$-$Cu_{40\%}$), ($W_{72\%}$-$Cu_{28\%}$). where it was compared with the available experimental values as well as the data of (APW)[1].In Figure 3, which shows the comparison between the theoretical values (calculations) of the Compton profile J(P_Z) for the values that have been extracted by adopting the (SUP) model and the values of (APW) with the experimental values adopted and given in Table 2 for alloys ($W_{60\%}$-$Cu_{40\%}$).

Now from Figure3, in the momentum region (0.0→0.3 a.u.), notice that the values of the Compton profile, based on the maximum superposition model, as well as the values of (APW) are somewhat close and equal to and different when compared with the experimental values[1]. In the moment. region (0.4 a.u.), notice that the values of the Compton profile, based on the greatest superposition model, are somewhat close and equal, in contrast to the values of (APW) when compared with the experimental values[1].In the momentum region (0.4→0.6a.u.), notice that the values of the Compton profile, based on the greatest superposition model, are the closest and are almost equal when compared with the experimental values. As for the values of the (APW) data, they are somewhat different when compared with the available experimental values[1].In the momentum region (0.7→1a.u), note that the Compton profile values, based on the superposition model, are closest and are approximately equal when compared to the experimental values. Invert Data Values (APW).in the momentum region (1.2 → 1.4a.u), note that the Compton profile values, based on

the largest overlay model of (APW) data values, are different among themselves when compared to the experimental values. As for the momentum region (1.4→2a.u.), notice that the values of the Compton profile, based on the greatest superposition model, as well as the values of (APW) are somewhat close and equal to each other and when compared with the experimental values[1].in the high momentum region (2→5a.u.) that all the values are approximately equal, because the electrons in this region are the core electrons only when compared with the experimental values[1].

Table 2: Our theoretical Compton profile results for (present work) were compared to the experimental values[1] and data (APW), These values Sup($W_{60\%}$-$Cu_{40\%}$)alloy were normalized to (18.2915) e^-.

P_z (a.u.)	$J(p_z)$ in (electron/a.u.)				
	COMPTON PROFILE: THEOR.			Data (APW)[1]	Expt.[1] ($W_{60\%}$-$Cu_{40\%}$)
	RFA (W) $5d^5$-$6s^1$	RFA (Cu) $3d^{9.9}$-$4s^{1.1}$	*Sup($W_{60\%}$-$Cu_{40\%}$)*		
0.0	9.394	5.222	7.725	7.84	7.48±0.0145
0.1	9.333	5.212	7.684	7.77	7.44
0.2	9.241	5.161	7.609	7.66	7.35
0.3	9.109	5.069	7.493	7.53	7.24
0.4	8.925	4.947	7.333	7.36	7.09
0.5	8.435	4.484	6.854	7.16	6.91
0.6	8.197	4.332	6.651	6.92	6.71
0.7	7.95	4.171	6.438	6.67	6.50
0.8	7.673	4.009	6.207	6.40	6.27
1.0	6.989	3.796	5.711	5.83	5.79±0.0120
1.2	6.296	3.654	5.239	5.27	5.32
1.4	5.732	3.422	4.808	4.75	4.90
1.6	5.237	3.13	4.394	4.29	4.49
1.8	4.782	2.839	4.004	3.92	4.13
2	4.444	2.558	3.689	3.61	3.79±0.0087
3	3.554	1.455	2.714	2.67	2.71±0.0066
4	2.843	0.912	2.070	2.07	2.05±0.0052
5	2.242	0.64	1.601	1.58	1.61±0.0043

Table 3: Our theoretical Compton profile results for (present work) were compared to the experimental values[1] and data (APW), These values Sup($W_{72\%}$-$Cu_{28\%}$)alloy were normalized to (20.4190) e^-.

P_z (a.u.)	J(p_z) in (electron/a.u.)				
	COMPTON PROFILE: THEOR.			Data (APW)[1]	Expt.[1] ($W_{72\%}$-$Cu_{28\%}$)
	RFA (W) $5d^5$-$6s^1$	RFA (Cu) $3d^{9.9}$-$4s^{1.1}$	*Sup($W_{72\%}$-$Cu_{28\%}$)*		
0.0	9.394	5.222	8.226	8.34	7.90±0.0148
0.1	9.333	5.212	8.179	8.26	7.88
0.2	9.241	5.161	8.099	8.15	7.83
0.3	9.109	5.069	7.978	8.01	7.72
0.4	8.925	4.947	7.811	7.84	7.57
0.5	8.435	4.484	7.329	7.62	7.38
0.6	8.197	4.332	7.115	7.38	7.17
0.7	7.95	4.171	6.892	7.11	6.94
0.8	7.673	4.009	6.647	6.83	6.68
1.0	6.989	3.796	6.095	6.22	6.14±0.0123
1.2	6.296	3.654	5.556	5.60	5.63
1.4	5.732	3.422	5.085	5.03	5.14
1.6	5.237	3.13	4.647	4.55	4.70
1.8	4.782	2.839	4.238	4.15	4.32
2	4.444	2.558	3.916	3.84	3.99±0.0089
3	3.554	1.455	2.966	2.91	2.99±0.0072
4	2.843	0.912	2.302	2.31	2.28±0.0058
5	2.242	0.64	1.793	1.78	1.81±0.0048

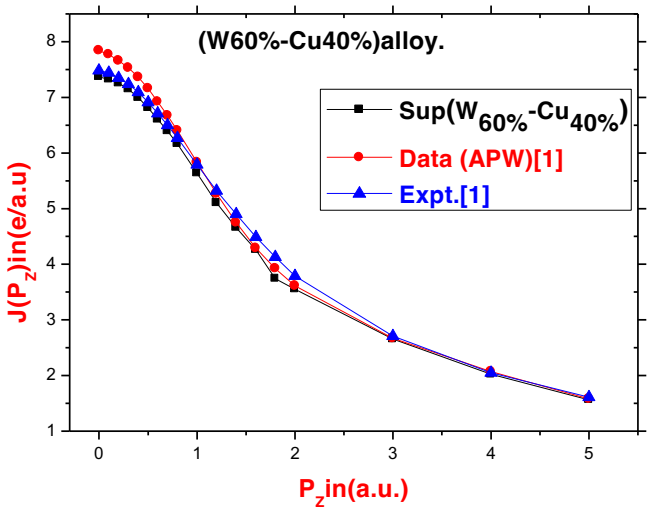

Fig.3: Comparison Compton J(P_Z) profile of the our theoretical values with experimental values[1] for the ($W_{60\%}$-$Cu_{40\%}$) alloy and Data (APW) ,all values were normalized to (18.2915) e^-.

In Figure4, which shows the comparison between the theoretical values (calculations) of the Compton profile J(P_Z) for the values that have been extracted by adopting the (SUP) model and the values of (APW) with the experimental values adopted and given in Tables 3 for Sup($W_{72\%}$-$Cu_{28\%}$), where better notice the equality and differences in Theoretical values extracted through the two models (SUP, APW) with experimental values[1]. Especially in the momentum region located between (2→5a.u.) This is due to the fact that the electrons in this region are the electrons of the core only , as well as in the momentum region located between (0.0→0.4a.u.) there is a great convergence between the values (SUP, APW). In the momentum region located between (0.6→1.6a.u.), also notice that there is a convergence in the values between them when compared with the available experimental values. also note from the two figures that the shapes are somewhat close. Whether it is compared with the available experimental values, and this means that the model used by us (SUP) works effectively and the results that obtain from it are acceptable results. This is the aim that we would like to reach and can prove that these mathematical models are effective and unique models.

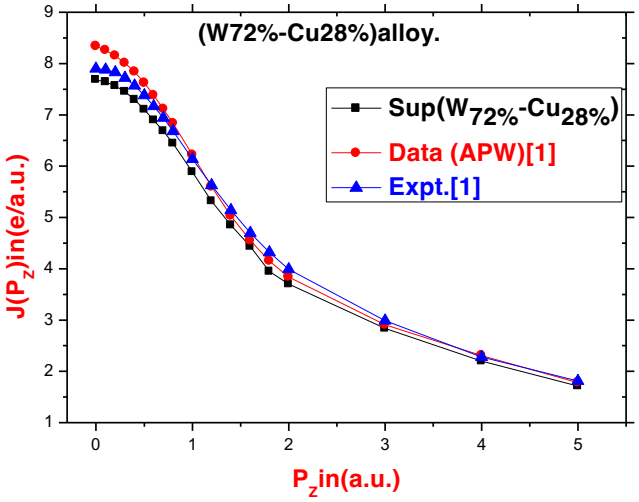

Fig.4: Comparison Compton J(P_Z) profile of the our theoretical values with experimental values[1] for the ($W_{72\%}$-$Cu_{28\%}$) alloy and Data (APW) ,all values were normalized to (20.4190) e^-.

Now to determine the best electronic configuration and examine the differences in the behavior of the two alloys, it is necessary to find the sum of the square of the difference between the theoretical and experimental values by applying the following relationship:

$$\left(\sum_0^5 \left(J_{Theo.}(p_z) - J_{exp.}(p_z)\right)\right)^2 = \sum_0^5 |\Delta J(p_z)|^2 \quad \textbf{(4)}$$

After referring to relation 4, the differences were found for the electronic configurations extracted by the superposition model.

Table 4: The difference between the values of theoretical calculations and experimental values for both alloys.

NO	Configuration	Different value
1	Sup($W_{60\%}$-$Cu_{40\%}$)alloy	0.444
2	Sup($W_{72\%}$-$Cu_{28\%}$)alloy	0.804

Figure.5 shows a plotted of the values resulting from this process, and note from Figure5 that the values of the electronic configuration Sup($W_{60\%}$-$Cu_{40\%}$)alloy is the closest to the experimental results from the electronic configuration Sup($W_{72\%}$-$Cu_{28\%}$)alloy, Where the sum of the difference between the theoretical and experimental values for both alloys was found by relation 4 and according to the following order: $\sum_0^5|\Delta J(p_z)|^2$ for [($W_{60\%}$-$Cu_{40\%}$)alloy{presentwork}(SUP)-expt.(CP)] and $\sum_0^5|\Delta J(p_z)|^2$ for [($W_{72\%}$-$Cu_{28\%}$)alloy{present work}(SUP)-expt.(CP)]. and the results were as in Table 4.Where notice from Fig.5 that the values of the configurations for both alloys are in the positive region for the momentum values that range between (P_Z = 0.0 → 0.5a.u.) and in the momentum region that ranges between (0.5 → 3a.u.) the values of the configurations are in the negative region and this result that obtained is almost harmonious order of with the figure in ref.1 , Figure5 shows a comparison plotted of the differences between the experimental and our theoretical (calculated) values of the (SUP) model, where clearly note that the differences are close for both alloys with the approved experimental results.

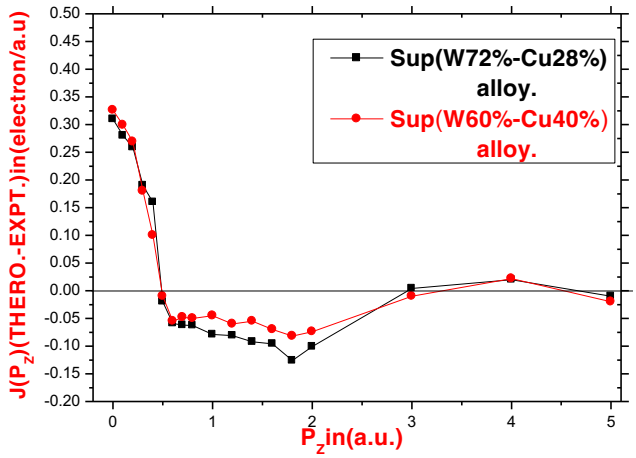

Fig.5: plotting a comparison of the differences between the practical values[1] and the theoretical (calculated) of the (SUP) model for the Sup($W_{60\%}$-$Cu_{40\%}$),($W_{72\%}$-$Cu_{28\%}$) alloy each The results have been normalized to (18.2915,20.4190) e^- respectively.

4. Conclusions

In this study, been study the Compton profile (CP) of:

W, Cu . elements and found best electronic configuration of the two elements they ($5d^5$-$6s^1$) and ($3d^{9.9}$-$4s^{1.1}$) respectively after it has been compared the results that have been obtained with the available experimental values,

($W_{60\%}$-$Cu_{40\%}$),($W_{72\%}$-$Cu_{28\%}$)alloys using the Superposition model and the results were compared with the available experimental values and (APW) data respectively, found Sup($W_{60\%}$-$Cu_{40\%}$)alloy was give a better agreement with available experimental values.

Acknowledgment. I'm grateful to the chairman and staff of physics department in the College of science UO.of Tikrit.

References

[1] Ahuja, B. L., et al., 2009, A study of electron momentum density and charge transfer in W–Cu system, Journal of alloys and compounds, 467(1-2), 595-599.

[2] Sharma, G., et al., 2011, Electron momentum density distribution in TiCu, Intermetallics, 19(5),666-670.

[3] Mendonça, J. T., and Haas, F. 2023, Compton scattering of plasmons, Physica Scripta, 98(6), 065603.

[4] Pazirandeh, Ali, and Maryam Azizi. 2010, Theoretical and experimental analysis of titanium Compton profile using ^{137}Cs, Applied Radiation and Isotopes 68.9: 1682-1686.

[5] James, A. D., et al., 2021, Magnetic Compton profiles of Ni beyond the one-particle picture: Numerically exact and perturbative solvers of dynamical mean-field theory, Physical Review B, 103(11), 115144.

[6] Khidzir, S. M., et al., 2017, GW approximation study of the Compton profile of ZnSe, Radiation Effects and Defects in Solids 172.7-8: 664-677.

[7] Khalaf, M., and Kaminer, I. 2023, Compton scattering driven by intense quantum light, Science Advances, 9(1), eade0932.

[8] Meena, S. K., et al., 2019, Performance of hybrid exchange-correlation potential for photocatalytic silver chromate and molybdate: LCAO theory and Compton spectroscopy, Physica B: Condensed Matter, 560, 236-243.

[9] Ruotsalainen, K. O., et al., 2018, The isotropic Compton profile difference across the phase transition of VO_2 , The European Physical Journal B, 91, 1-6.

[10] Aguiar, J. C., et al., 2017, Theoretical Compton profile of diamond, boron nitride and carbon nitride, Physica B: Condensed Matter, 521, 361-364.

[11] Aguiar, J. C., et al., 2013, Experimental Compton profiles of Be, Al and Ti and comparisons to generalized gradient approximation calculations, Journal of Physics and Chemistry of Solids, 74(10), 1341-1348.

[12] Varghese, T., and Balakrishna, K. M.,2010, Electron momentum distribution and

Compton profiles of europium, The European Physical Journal D, 57, 9-11.

[13] Ahuja, B. L., et al., 2006, Compton profile study of tin, physica status solidi (b), 243(3),625-634.

[14] Varghese, T., et al., 2003, Compton profile of tantalum, Pramana, 60, 569-573.

[15] Meena, S. K., and Ahuja, B. L. 2018, Electronic structure and electron momentum densities of Ag_2CrO_4, In AIP Conference Proceedings (V.1953, N.1).

[16] Sahariya, Jagrati, and B. L. Ahuja. 2012, Electronic structure of Ni_2TiAl: Theoretical aspects and Compton scattering measurement, Physica B: Condensed Matter 407.21:4182-4185.

[17] Kaliman, Z., et al., 2011, Compton scattering from positronium and validity of the impulse approximation, Physical Review A, 83(5), 053406.

[18] Joshi, R., et al., 2011, Compton scattering study and electronic properties of vanadium carbide: A validation of hybrid functional, Physica B: Condensed Matter 406.10: 2007-2012.

[19] Bansil, A., et al., 1998, Compton study of $Ni_{75}Cu_{25}$ and $Ni_{75}Co_{25}$ disordered alloys: Theory and experiment, Physical Review B, 57(1),314.

[20] Heda, N. L., et al. 2010, Electronic properties and Compton profiles of molybdenum dichalcogenides, Journal of Physics and Chemistry of Solids 71.3: 187-193

[21] Khera, S., et al., 2007, Electronic structure of hafnium: A Compton profile study, Pramana 68: 91-98.

[22] Ahuja, B. L., et al., 1998, Compton study of the electronic state in Fe–Ni alloys, Physica Scripta, 58(2), 185.

[23] Sharma, G., et al. 2011, Compton profile and charge transfer study in intermetallic Ti–Al system, Intermetallics 19.8 :1107-1114.

[24] Pal, D., and Padhi, H. C. 1993, Compton Profile Studies of Cr_xNi_{1-x} Alloys, physica status solidi (b), 175(2),507-512.

[25] Pal, D., and Padhi, H. C. 1992, Compton Profile Studies of Ti_xNi_{1-x} Alloys, physica status solidi (b), 65 (3), 553-558.

[26] Rathor, A., et al., 2008, Band-structure calculations and electron momentum densities of AgCl and AgBr, physica status solidi (b), 245(8), 1563-1570.

[27] Ahmed, G., et al., 2009, Electronic properties of $PbCl_2$ and $PbBr_2$ using Compton scattering technique, Applied Radiation and Isotopes, 67(6), 1050-1056.

[28] Dobrzynski, L., et al., 2001, A Compton Scattering Study of Charge Transfer in Cr-Fe-Mn Alloys, 215, 11, 1389–1395.

[29] Berggren, K. F. 1972, Renormalized-Free-Atom Model and the Electron Momentum

Distribution in Vanadium, Physical Review B, 6(6), 2156.

[30] Hodges, L., et al., 1972, Renormalized atoms and the band theory of transition metals, Physical Review B, 5(10), 3953.

[31] Fischer, C. F. 1972, Average-Energy-of-Configuration Hartree-Fock Result for the Atoms Helium to Radon, Atomic Data, 4, 301.

[32] Clementi, E., and Roetti, C. 1974, Roothaan-Hartree-Fock atomic wave functions : Basis functions and their coefficients for ground and certain excited states of neutral and ionized atoms, Z≤ 54. Atomic data and nuclear data tables, 14(3-4), 177-478.

[33] Biggs, F., et al., 1975, Hartree-Fock Compton profiles for the elements, Atomic data and nuclear data tables, 16(3), (201-309.